AACR 2023 Abstract#4688

Comprehensive analysis of natural killer cell - associated markers using MultiOmyx™ immunofluorescence assay

Erinn A. Parnell • Jiong Fei • Harry Nunns • Eric Leones • Elaine Yeung • Blair Russell • Flora Sahafi • Qingyan Au

NeoGenomics Laboratories, Aliso Viejo, CA

As a promising alternative platform for cellular immunotherapy, natural killer cells (NK) have recently gained attention as an important type of innate immune regulatory cell. NK cell immunotherapy approaches have been translated into clinical applications, and clinical trials of NK cell infusion in patients with hematological malignancies (HM) and solid tumors have thus far yielded many encouraging clinical results. Understanding the pattern of NK expression and the relationship to different states of NK cells may have direct relevance for immune responses in cancer. Approaches capable of simultaneously detecting NK cells with detailed information on NK differentiation state, however, remain limited.

In this study, we used MultiOmyx hyperplexed immunofluorescence (IF) assay to classify and characterize the spatial arrangement of NK cell markers in a pan-cancer cohort including 6 tissue microarrays (TMAs) from prostate, colon and lung cancer indications. The panel includes CD3, CD4, CD8, CD16, CD45, CD56, CD57, CD137, FoxP3, Granzyme B, HLA-E, NKG2A, NKP46 and tumor segmentation marker. The panel enables the detection of NK cells expressing CD56 and/or NKP46 in the 3 different tumor indications. We also studied the expression of activating and inhibiting receptors, such as CD16 and NKG2A, in NK cell population. The actively cytotoxic subsets of mature NK cells were evaluated using co-expression of NK cell surface markers with CD57 and the cytotoxic molecule expression in NK cells was assessed using co-expression with Granzyme B. Using proprietary deep-learning-based image analysis, we were able to quantify the densities of these different NK cell population and study the prevalence of these NK cells in different cancer indications included in this study.

Many strategies have been developed for exploiting NK-mediated anti-tumor activities. CAR-NK cell therapy and antibodies that directly target NK cell inhibitory receptors such as NKG2A and TIGIT, are currently being evaluated in the clinical trials. The MultiOmyx NK cell panel reported in this study enables the comprehensive profiling of the NK population and can provide greater understanding of NK cell biology during cancer progression. The panel can be further used to explore the efficacy of the NK cell-based immune therapy.

MultiOmyx Assay Workflow and Biomarker Panel

A

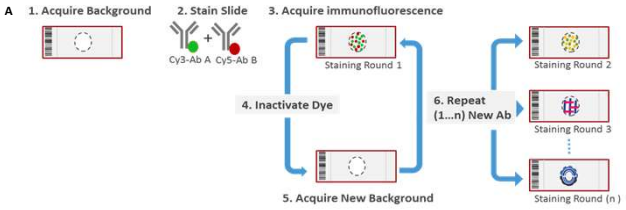

Figure 1. A. MultiOmyx Assay Workflow. Each sample was analyzed by MultiOmyx IF assay. For MultiOmyx IF study, slides were prepared and stained using MultiOmyx multiplexing IF staining protocol. For each round of staining, conjugated fluorescent antibodies were applied to the slide, followed by imaging acquisition of stained slides. The dye was erased, enabling a second round of staining with another pair of fluorescent antibodies. **B. Table 1.** Biomarkers included in NK discovery panel. **Table 2.** Phenotypes of T and NK populations and tumor cells.

B

MultiOmyx NK Panel Biomarkers and Representative Phenotypes

Panel Biomarkers
CD16
CD3
CD4
CD8
CD45
CD56
CD57
CD137
FoxP3
GranzymeB
HLA-E
NKG2A
NKP46
PanCK

Co-expression	Phenotypes	Co-expression	Phenotypes
CD3+CD4+	T helper cells	CD16+CD56+	NK cells
CD3+CD4+FoxP3+	T regulatory cells	CD16+NKP46+	NK cells
CD3+CD8+	T cytotoxic cells	CD56+GranzymeB+	GZMB+ NK cells
CD3+CD8+GranzymeB+	GZMB+ T cytotoxic cells	NKP46+GranzymeB+	GZMB+ NK cells
CD57+CD3+	CD57+ T cells	CD3+CD56+	NKT cells
CD57+CD3+CD4+	CD57+ T helper cells	CD3+NKP46+	NKT cells
CD57+CD3+CD8+	CD57+ T cytotoxic cells	CD57+CD56+	CD57+ NK cells
CD137+CD3+	CD137+ T cells	CD57+NKP46+	CD57+ NK cells
CD137+CD3+CD4+	CD137+ T helper cells	CD137+CD56+	CD137+ NK cells
CD137+CD3+CD8+	CD137+ T cytotoxic cells	CD137+NKP46+	CD137+ NK cells
NKG2A+CD3+	NKG2A+ T cells	NKG2A+CD56+	NKG2A+ NK cells
NKG2A+CD3+CD8+	NKG2A+ T cytotoxic cells	NKG2A+NKP46+	NKG2A+ NK cells
HLA-E+CD45+	HLA-E+ immune cells	HLA-E+PanCK+	HLA-E+ tumor cells

Comprehensive Analysis of NK-associated Markers Using MultiOmyx Assay

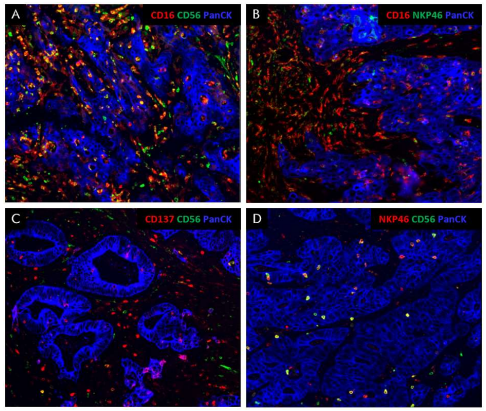

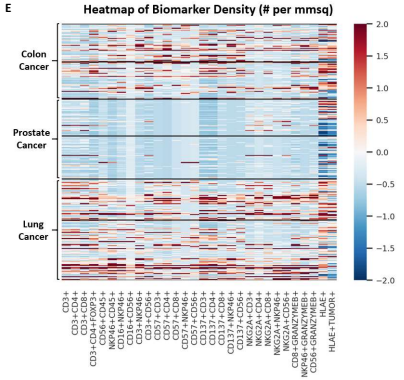

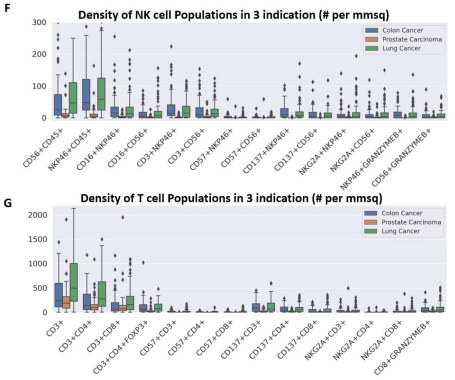

Figure 2: Characterization of T and NK cell populations in colon, prostate and lung cancers. A-D. Representative color overlay images showing expression of NK cells in colon and lung carcinoma specimens (tumor cells in blue). (A) Co-expression of CD16+CD56+ cells in yellow (colon). (B) Co-expression of CD16+NKP46+ cells in yellow (lung). (C) Co-expression of NKP46+CD56+ cells in yellow (colon). (D) Co-expression of CD137+CD56+ cells in yellow (colon). **E.** Heat map of MultiOmyx cell classification results in 3 cancer types. The results of each biomarker and co-expression are given in densities (# per mmsq). **F.** Boxplots comparing the densities of NK phenotyping, modulating, and effector biomarkers in colon, prostate, and lung cancer TMA samples. **G.** Boxplots comparing the densities of T cell subsets in colon, prostate, and lung cancer TMA samples.

Quantification of NK-associated Markers Using Proprietary Deep-learning Based Analytics Pipeline

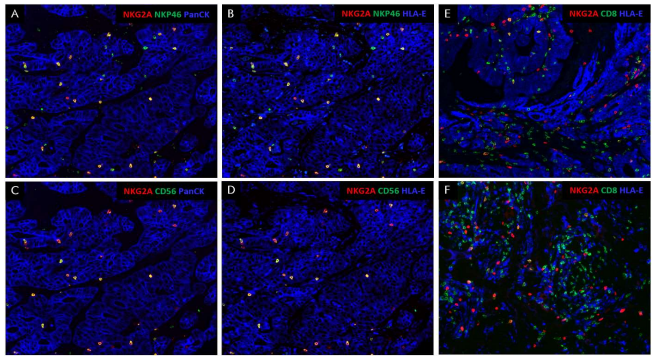

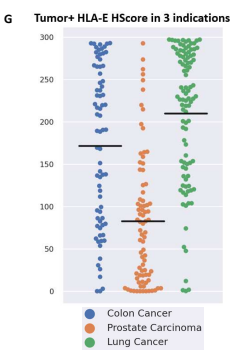

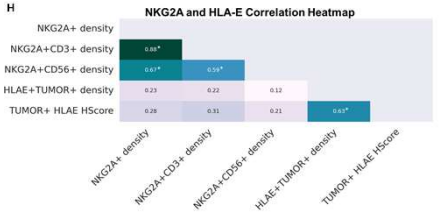

Figure 3: Characterization of inhibitory signaling through NKG2A-HLA-E axis in NK and T cells in colon, prostate, and lung carcinomas. A-F. Representative color overlay images showing expression of NKG2A on NK and T cells and HLA-E expression in colon and lung carcinoma specimens. **(A-B)** Co-expression of NKG2A+NKP46+ cells in yellow with PanCK+ tumor or HLA-E expressing cells in blue (colon). **(C-D)** Co-expression of NKG2A+CD56+ cells in yellow with PanCK+ tumor or HLA-E expressing cells in blue (colon). **(E-F)** Co-expression of NKG2A on cytotoxic T cells in yellow and HLA-E in blue (E, colon, F, lung). **G.** Swarmplots of HLA-E HScore for tumor HLA-E expression in colon, prostate, and lung carcinomas. **H.** Correlation heatmap of HLA-E HScore and NKG2A density on NK and T cells from pooled data from colon, lung, and prostate carcinomas. . Spearman correlations were averaged across the three indications, and considered significant (*) if the p value < .05.

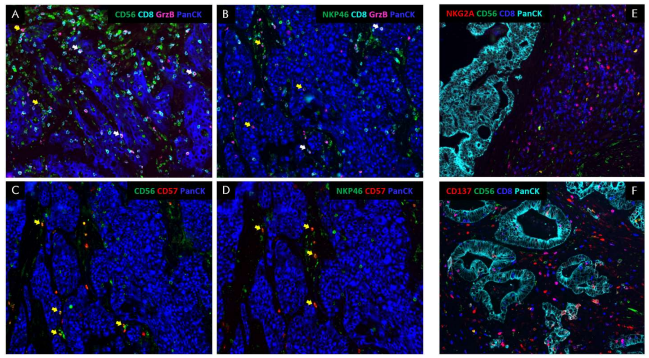

Figure 4: Comparison of inhibitory and co-stimulatory molecules on T and NK cells.
A-F. Representative color overlay images showing expression of Granzyme B in colon carcinoma (A-B) and CD57 in lung cancer (C-D) specimens. (A) Co-expression of GrzB on CD56+ (yellow arrows) or CD8+ (white arrows) cells. (B) Co-expression of GrzB on NKP46+ (yellow arrows) or CD8+ (white arrows) cells. (C) Co-expression of CD56+CD57+ cells in yellow. (D) Co-expression of NKP46+CD57+ cells in yellow.
(E) Representative color overlay image showing expression of NKG2A on CD56+ cells (yellow) and cytotoxic T cells (CD8+, magenta) in prostate carcinoma.
(F) Representative color overlay image showing expression of CD137 on CD56+ cells (yellow) and cytotoxic T cells (CD8+, magenta) in colon carcinoma.

Key Findings

- MultiOmyx panel utilizing NK-specific markers allows for comprehensive profiling of NK subsets as well as their modulating receptors.
- NK cells were more abundant in colon and lung cancers than prostate cancers in the samples analyzed. T cells showed this trend, but to a lesser degree.
- HLA-E HScore was higher in lung and colon cancers than prostate cancers. No specific correlation was found between higher expression of NKG2A in either NK or T cells and the density of HLA-E in this study.